Electronic Supplementary Material (ESI) for Dalton Transactions.
This journal is © The Royal Society of Chemistry 2016

Supporting Information

Amide bond cleavage initiated by coordination with transition metal ions and tuned by an auxiliary ligand

Yongpo Yang[a], Chunxin Lu[b], Hailong Wang[b], Xiaoming Liu[b*]

[a]School of Petrochemical Engineering,Changzhou University, Changzhou 213164,China

[b]College of Biological, Chemical Sciences and Engineering, Jiaxing University, Jiaxing 314001, China

*Corresponding author, Email: xiaoming.liu@mail.zjxu.edu.cn; xiaoming.liu@ncu.edu.cn; Tel./Fax: +86 (0)573 83643937

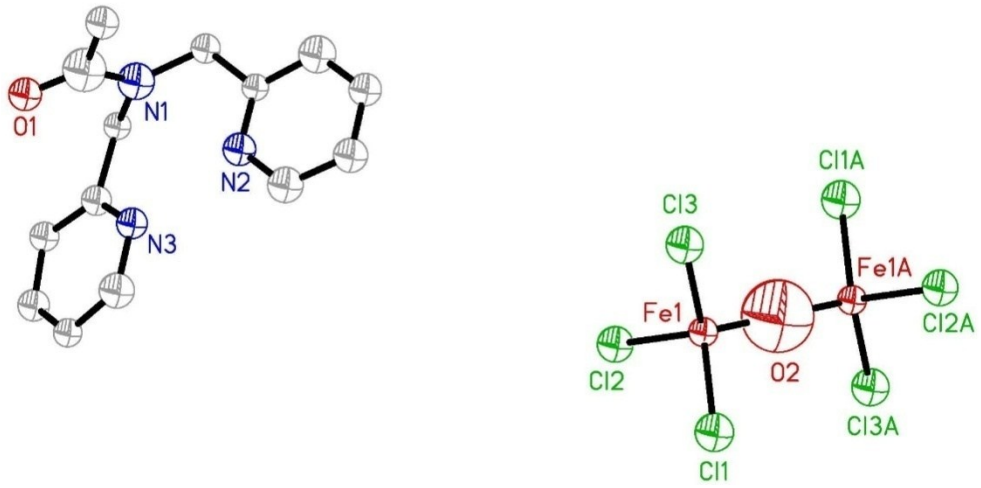

Fig. S1 The structure of dication $[Fe_2(\mu\text{–}O)Cl_3]^{2-}$ with protonated ligand ($H_2\mathbf{L}^{2+}$) as its counter ion.

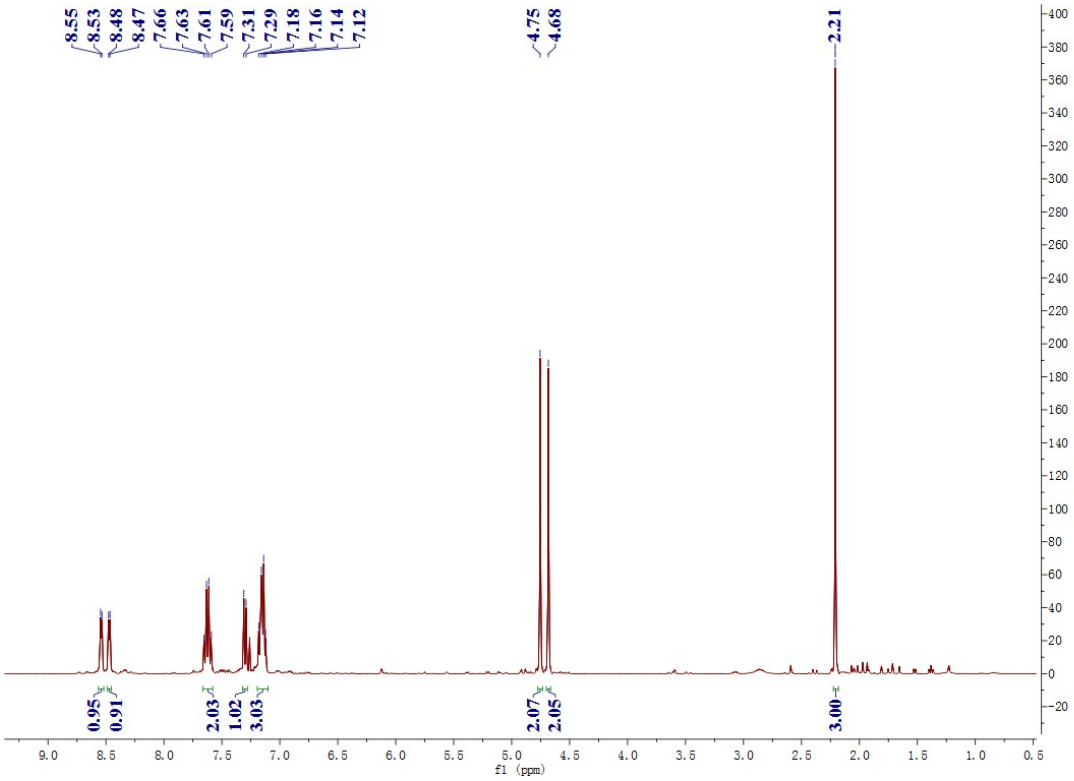

Fig. S2 ^{1}H NMR spectrum of the product isolated from the acidification of complex **1** ($CDCl_3$).

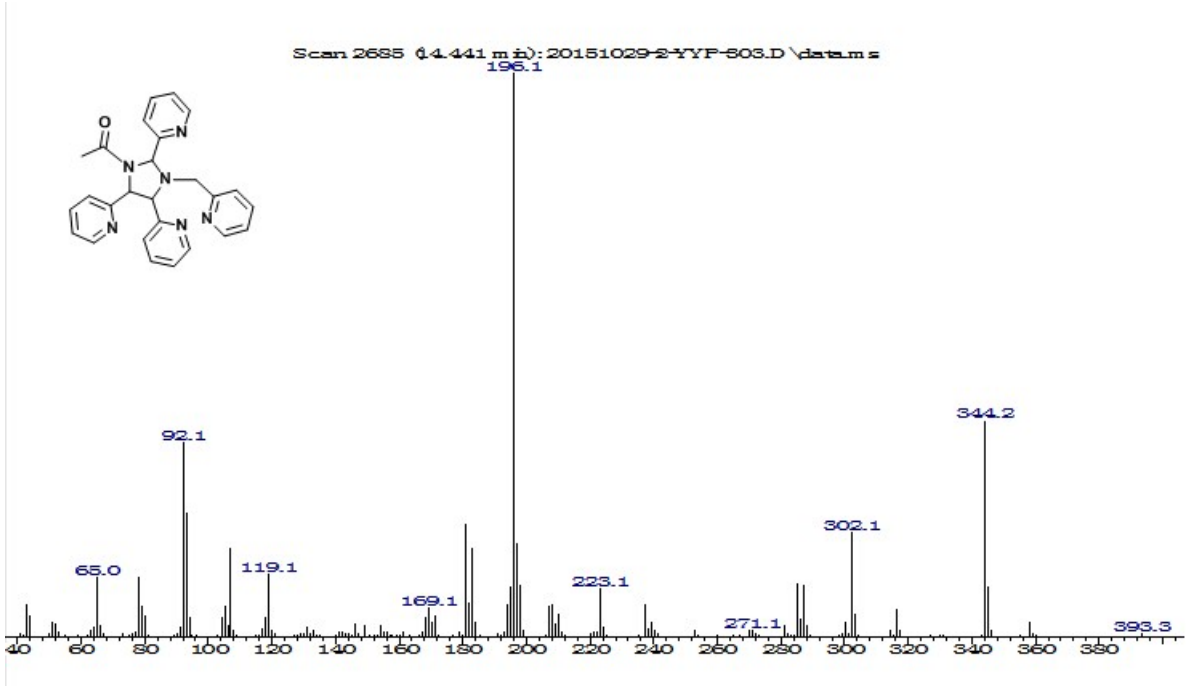

Fig. S3 GC-MS spectrum of the extract of the acidified solution of complex **1** by CH_2Cl_2.

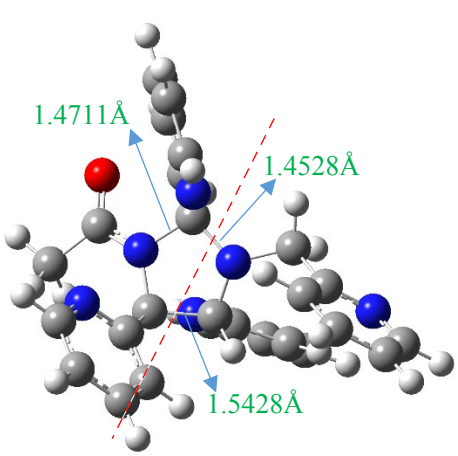

Ligand **L'** (top view)

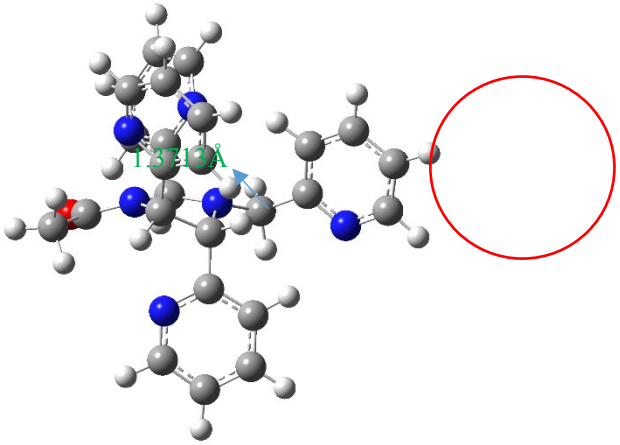

Ligand **L'** (side view)

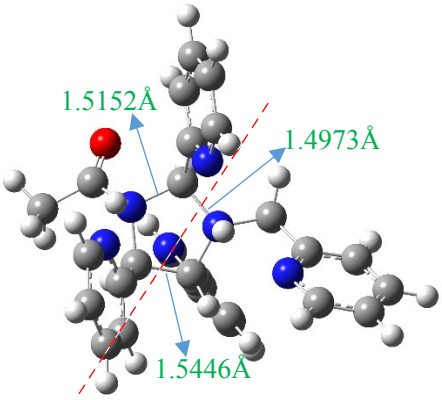

Protonated ligand H_2**L'**$^{2+}$ (top view)

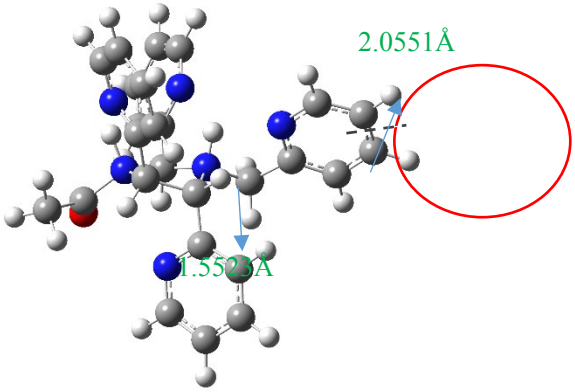

Protonated ligand H_2**L'**$^{2+}$ (side view)

Fig. S4 The selected structural parameters of the optimised structures of ligand **L'** and its protonation $\mathbf{H_2L'^{2+}}$.

The structures of ligand **L'** and its protonation on thetwo N atoms of the five-member heterocyclic ring $\mathbf{H_2L'^{2+}}$ were fully optimised in gas phase without any symmetry constraints using B3LYP method with the 6-31G(d,p) basis set. Vibrational frequencies were calculated and the absence of negative frequencies confirmed that the structures were local minimum energy structures. All the calculated were carried out using Gaussian 03 program[1]. The optimised structures are displayed in **Fig. S4**,

the calculated results show that the central pentacyclic ring of protonated ligand H_2**L'**$^{2+}$ was not open through C-C and C-N bond clearage to give ligand L and its deacetylation product according to our speculation. The bond lengths of C-C and C-N vary slightly from 0.0018 Å to 0.0445 Å. But the amido bond becomes longer (0.1810 Å), it indicated that the protonation of ligand **L'** may induced deacetylation. Another significantly change of $\mathbf{H_2L'^{2+}}$is that the pyridine ring rotation around the C-C single bond to form intra-molecular hydrogen bond. The N···H distance (2.0551 Å) is significantly shorter than the sum of the van der Waals radii of O and H atoms (2.75Å)[2].

Reference:

[1] M.J.Frisch, G.W. Trucks H.B. Schlegel, G.E. Scuseria, M.A. Robb, J.R. Cheeseman, J.A. Jr. Montgomery, T. Vreven, K.N. Kudin, J.C. Burant, J.M. Millam, S.S. Iyengar, J. Tomasi, V. Barone, B. Mennucci, M. Cossi, G. Scalmani, N. Rega, G.A. Petersson, H. Nakatsuji, M. Hada, M. Ehara, K. Toyota, R. Fukuda, J. Hasegawa, M. Ishida, T. Nakajima, Y. Honda, O, Kitao, H. Nakai, M. Klene, X. Li, J.E. Knox, H.P. Hratchian, J.B. Cross, V. Bakken, C. Adamo, J. Jaramillo, R Gomperts, R.E. Stratmann, O. Yazyev, A.J. Austin, R. Cammi, C. Pomelli, J.W. Ochterski, P.Y. Ayala, K. Morokuma, G.A. Voth, P. Salvador, J.J. Dannenberg, V.G. Zakrzewski, S. Dapprich, A.D. Daniels, M.C. Strain, O. Farkas, D.K. Malick, A.D. Rabuck, K. Raghavachari, J.B. Foresman, J.V. Ortiz, Q. Cui, A.G. Baboul, S. Clifford, J. Cioslowski, B.B. Stefanov, G. Liu, A. Liashenko, P. Piskorz,I. Komaromi, R.L. Martin, D.J. Fox, T. Keith, M.A. Al-Laham, C.Y. Peng, A. Nanayakkara, M. Challacombe, P.M.W. Gill, B. Johnson, W. Chen, M.W. Wong, C. Gonzalez, J.A. Pople, Gaussian 03, Revision E.01; Gaussian Inc., Wallingford, CT, 2003.

[2] A. Bondi, van der waals volumes and radii, *J. Phys. Chem*., 1964,**68**, 441-451.

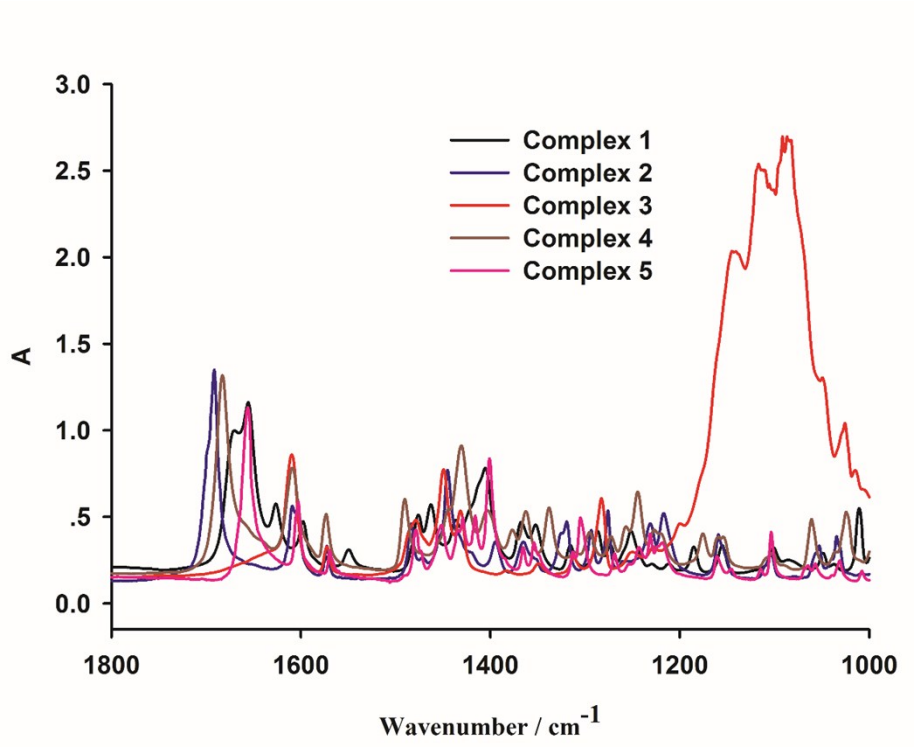

Fig. S5 IR spectra of complexes **1**-**5** at room temperature (**1**: ν_{CO} = 1655 cm^{-1}; **2**: ν_{CO} =1691 cm^{-1}; **4**: ν_{CO} = 1682 cm^{-1}; **5**: ν_{CO} = 1656 cm^{-1}; **3**: ν_{ClO4^-} = 1170-1050 cm^{-1}).

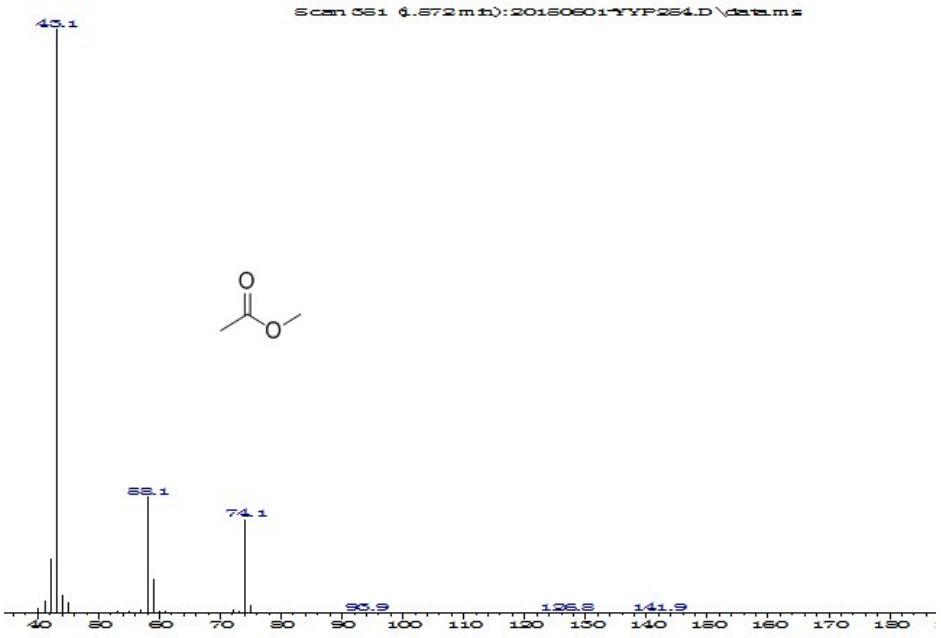

Fig. S6 GC-MS of the reaction solution after the isolation of the major product (**3**) in CH_3OH.

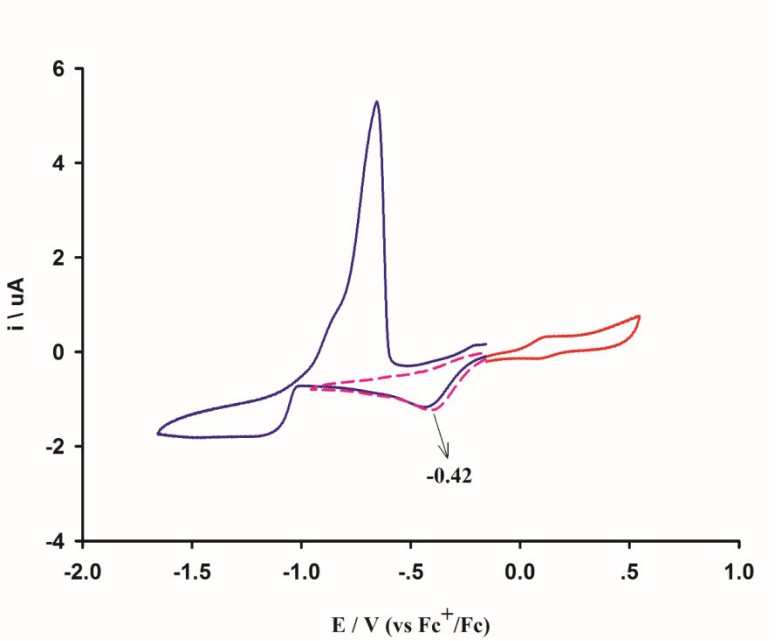

Fig. S7 Cyclic voltammograms of complex **2** (3.2 mmol L^{-1}) in 0.1 mol L^{-1} [N^nBu$_4$]BF_4–CH_3CN under an Ar atmosphere (298 K, scanning rate = 100 mV s^{-1}).

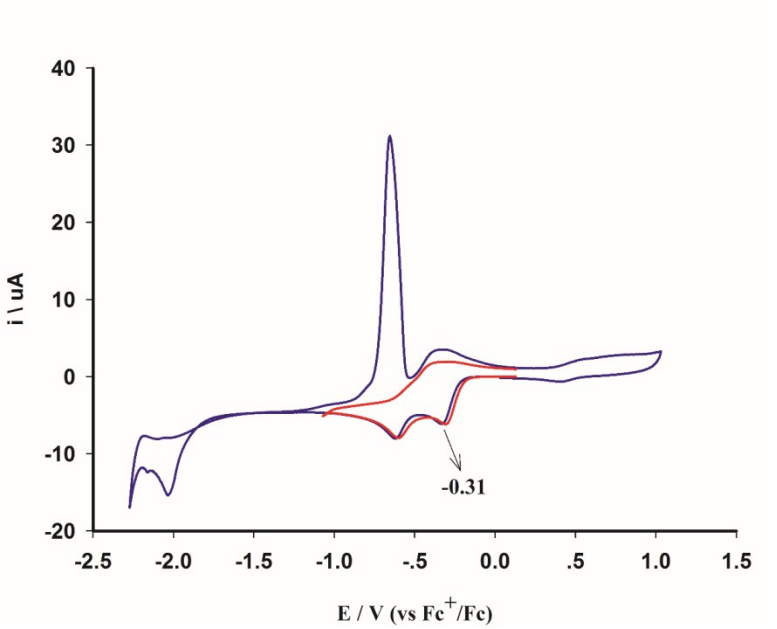

Fig. S8 Cyclic voltammograms of complex **3** (3.2 mmol L^{-1}) in 0.1 mol L^{-1} [N^{n}Bu$_4$]BF_4–CH_3CN under an Ar atmosphere (298 K, scanning rate = 100 mV s^{-1}).

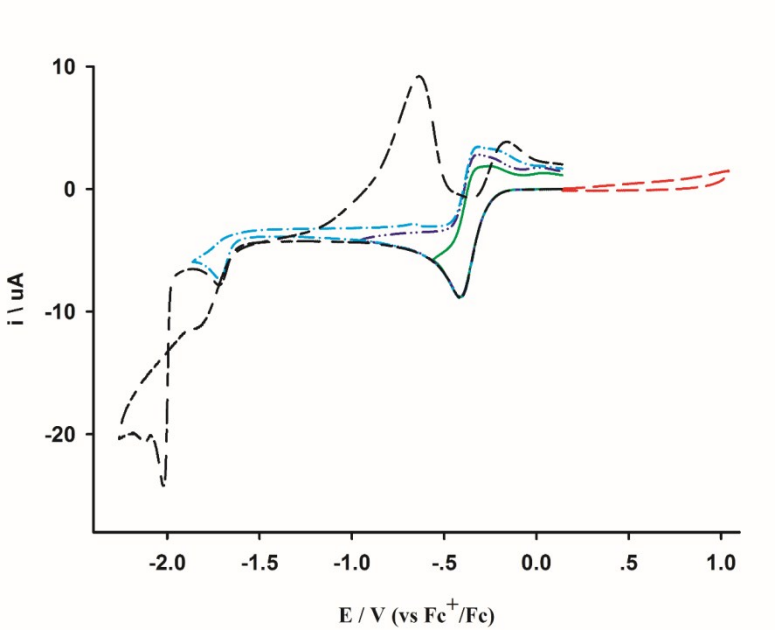

Fig. S9 Cyclic voltammograms of complex **1** (3.2 mmol L^{-1}) in 0.1 mol L^{-1} [N^nBu$_4$]BF_4–CH_3CN under an Ar atmosphere (298 K, scanning rate = 100 mV s^{-1}).

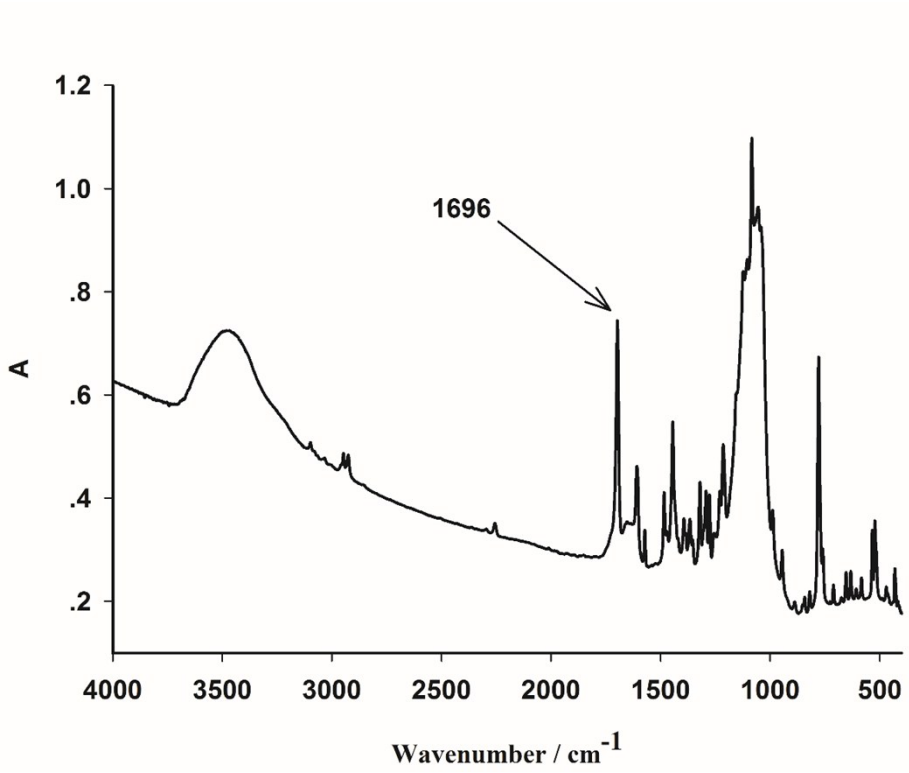

Fig. S10 The IR spectrum of the product from the reaction of complex **2** with $AgBF_4$ in acetonitrile (KBr pellet).

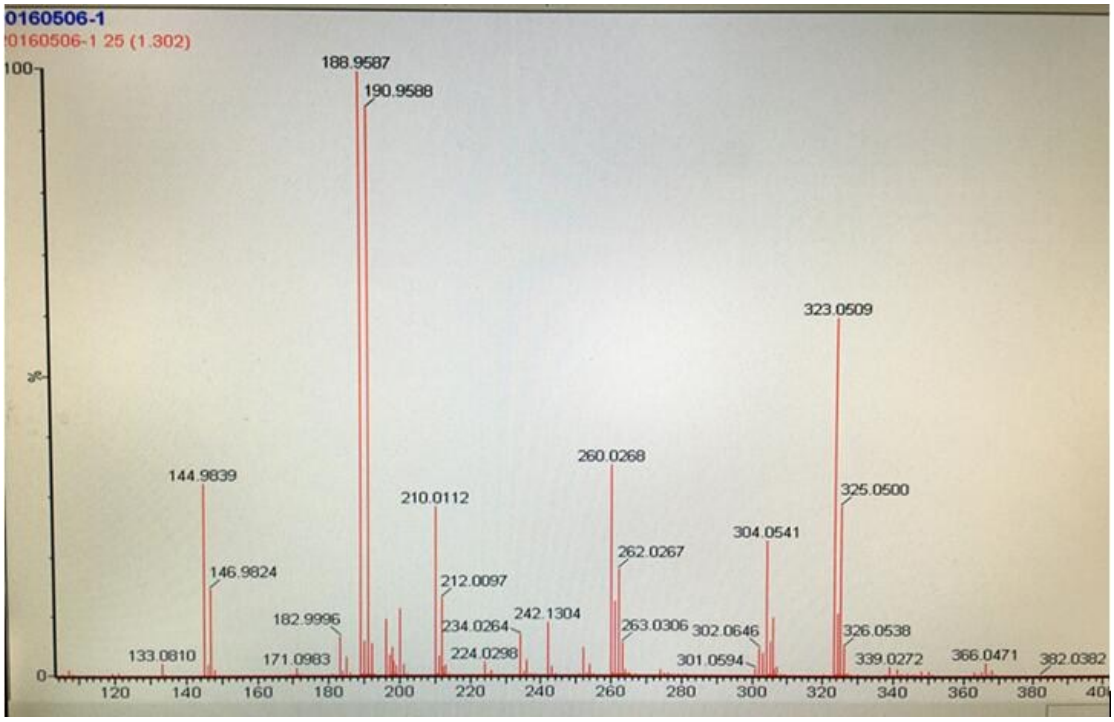
0160506-1
0160506-1 25 (1.302)
100
%
0
188.9587
190.9588
323.0509
260.0268
144.9839
210.0112
325.0500
304.0541
262.0267
146.9824
212.0097
182.9996
242.1304
234.0264
263.0306
302.0646
326.0538
133.0810
171.0983
224.0298
301.0594
339.0272
366.0471
382.0382
120 140 160 180 200 220 240 260 280 300 320 340 360 380

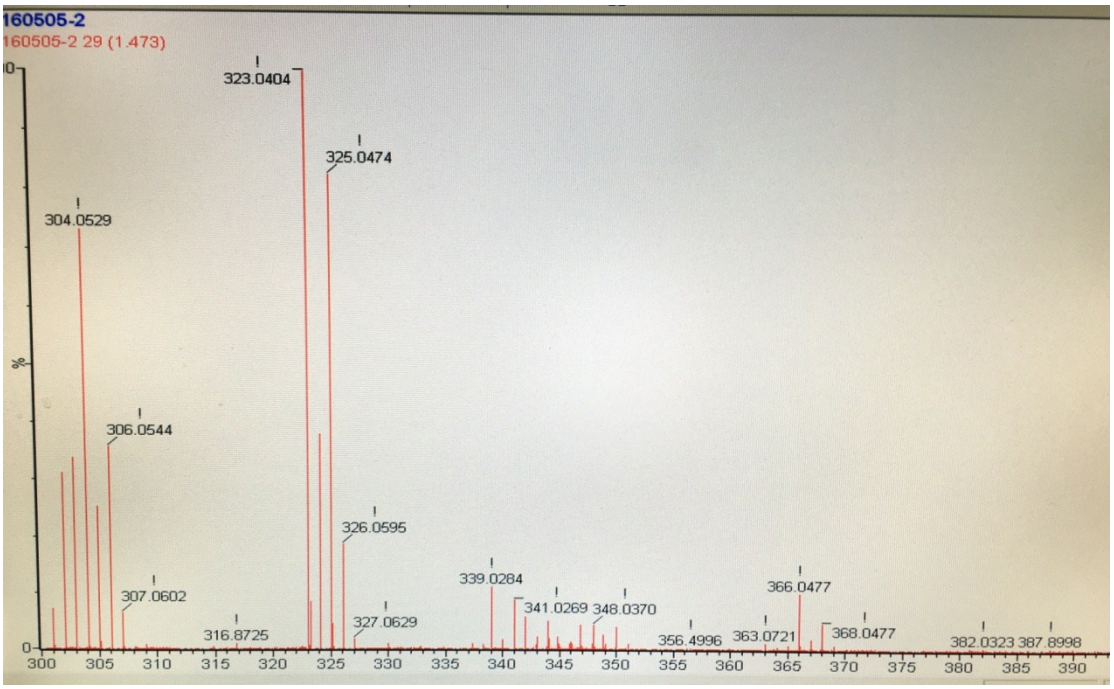
160505-2
160505-2 29 (1.473)
%
0
323.0404
325.0474
304.0529
306.0544
326.0595
339.0284
366.0477
307.0602
341.0269
348.0370
316.8725
327.0629
356.4996
363.0721
368.0477
382.0323 387.8998
300 305 310 315 320 325 330 335 340 345 350 355 360 365 370 375 380 385 390

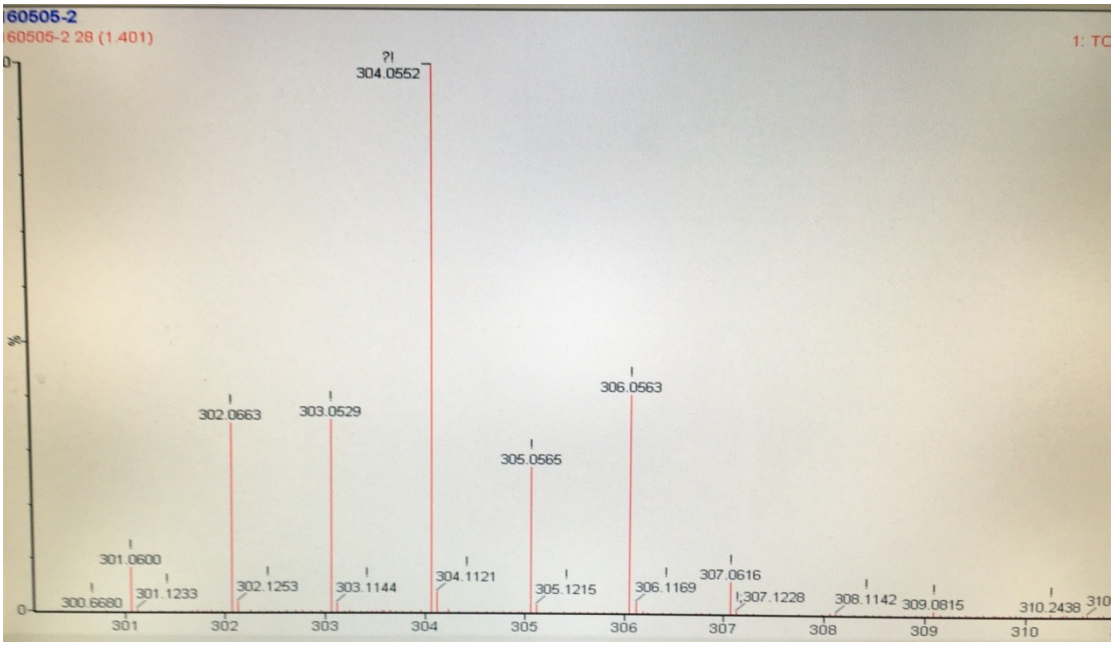

Fig. S11 MS spectra of the product from the reaction of complex **2** with $AgBF_4$ in CH_3CN.

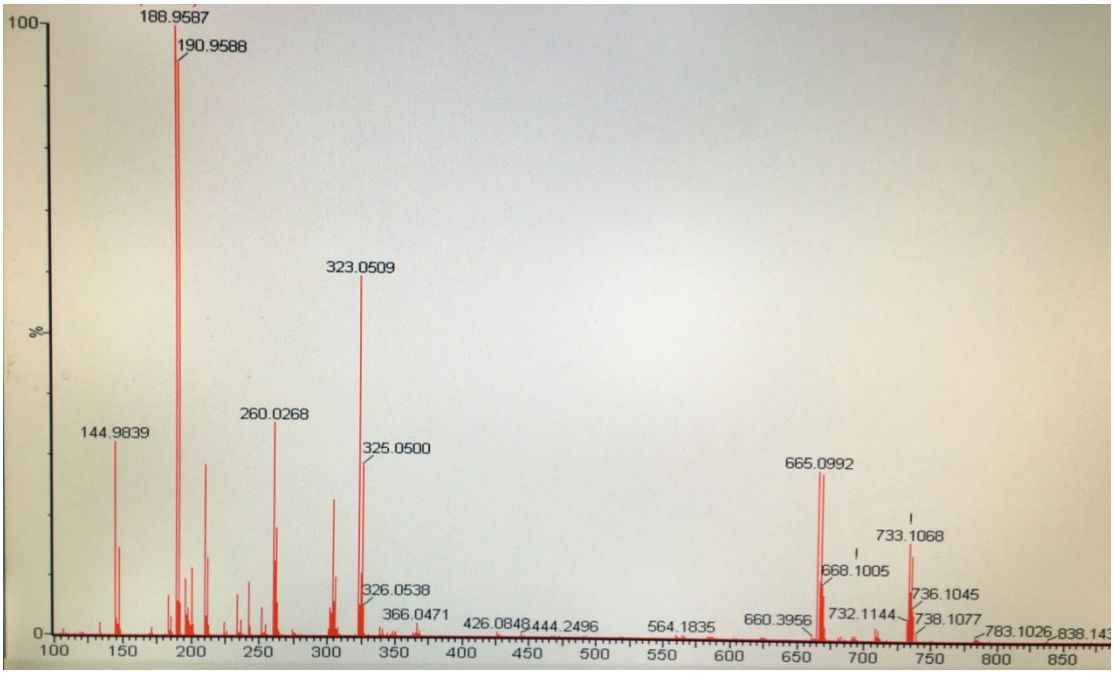

Fig. S12 MS spectra of the reaction of complex **2** with $AgBF_4$ in CH_3CN after filtering off AgCl.

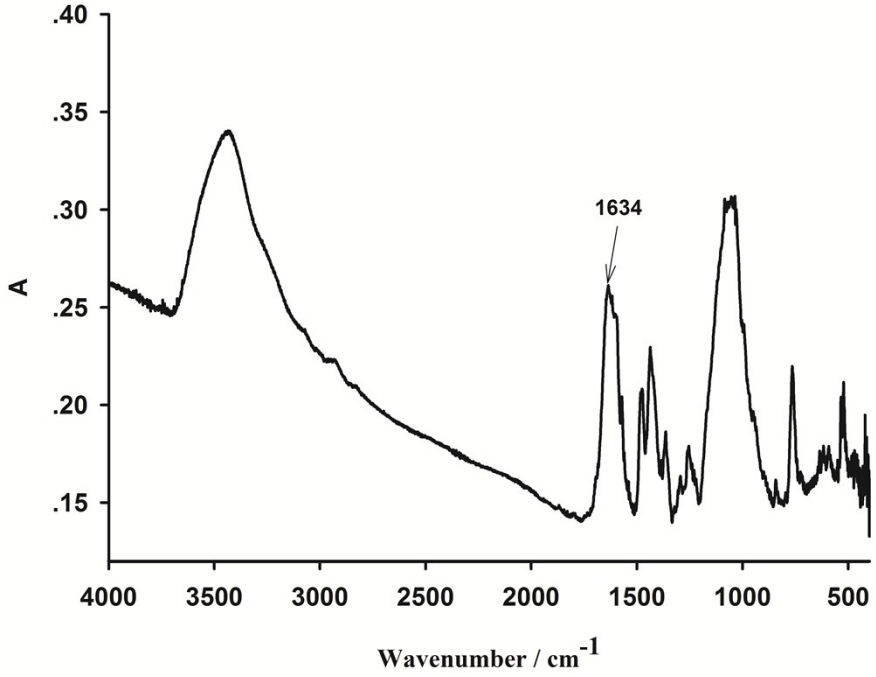

Fig. S13 The IR spectrum of the product from the reaction of complex **2** with $AgBF_4$ in methanol (KBr pellet).

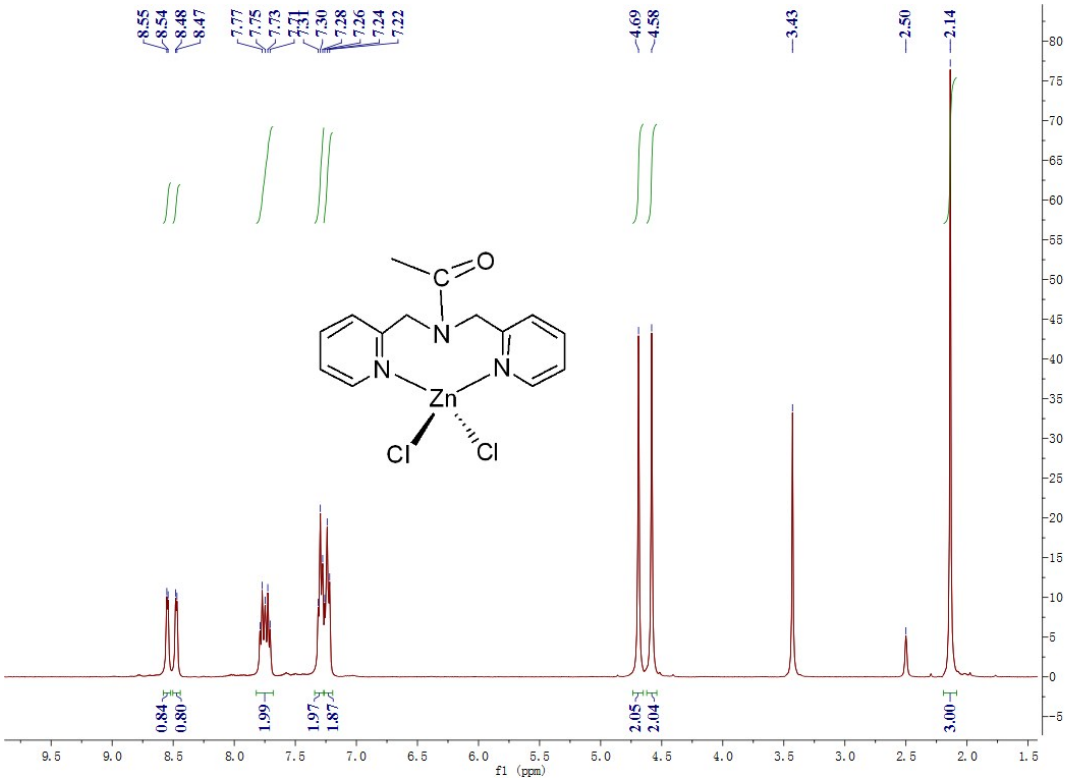

Fig. S14 ^1H NMR spectrum of complex **4** (DMSO-d_6).

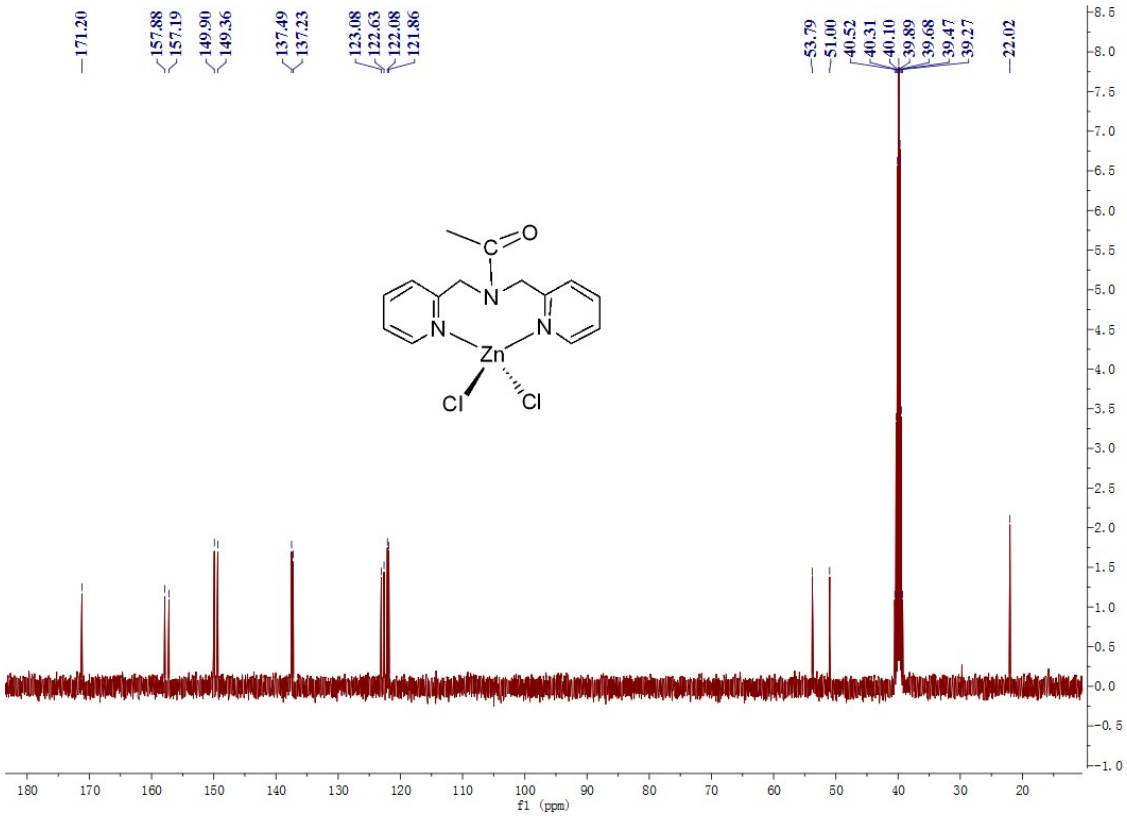

Fig. S15 ^{13}C NMR spectrum of complex **4** examined (DMSO-d_6).

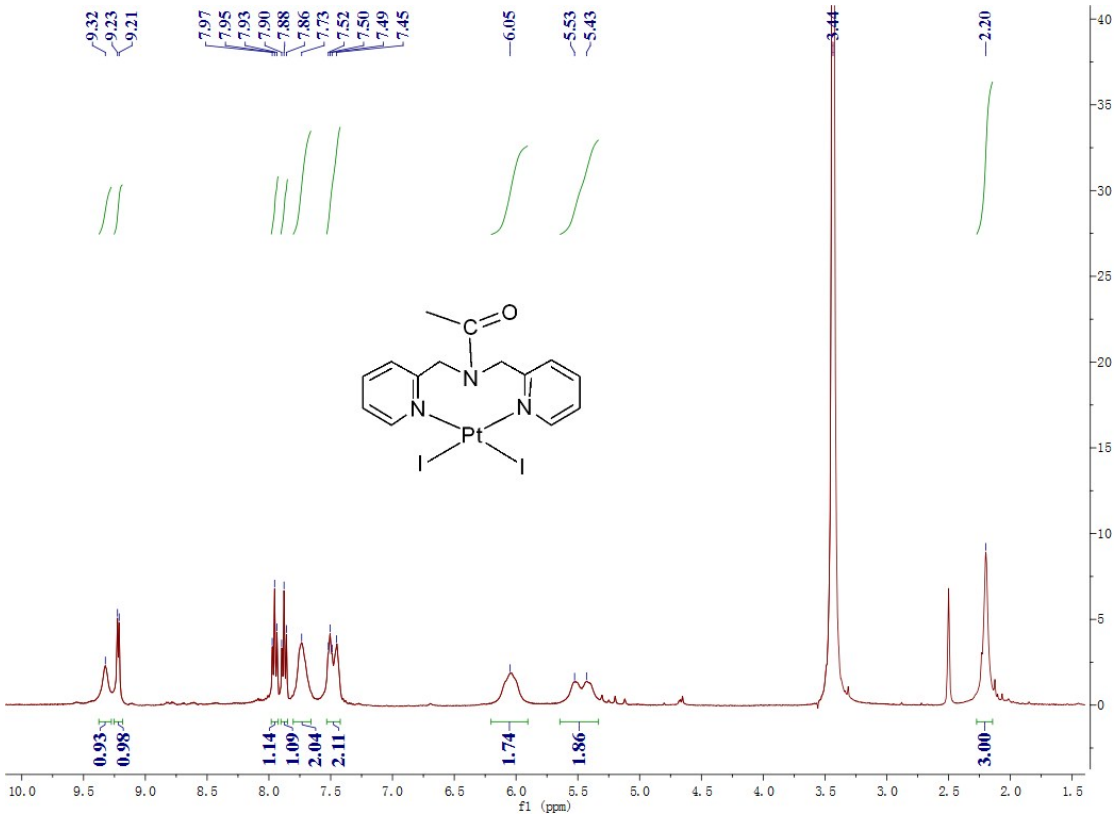

Fig. S16 ^{1}H NMR spectrum of complex **5** (DMSO-d_6).

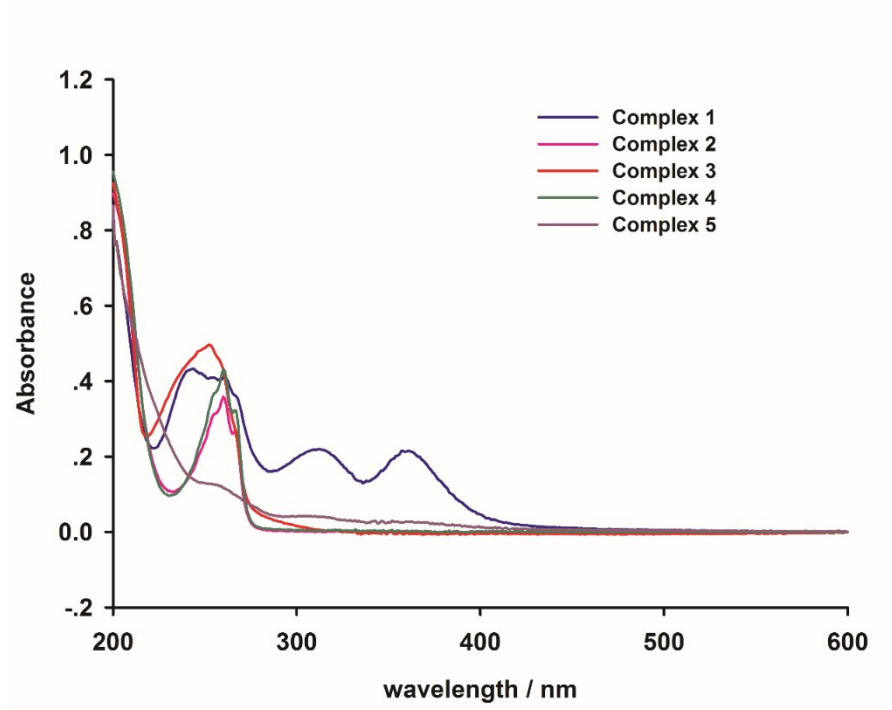

Fig. S17 UV-vis spectra of complexes **1-5** (CH_3CN).